06.1;06.5

Distribution of mechanical properties in annual growth rings of deciduous trees measured using scanning nanoindentation

© Yu.I. Golovin[1,2], A.I. Tyurin[1], A.A. Gusev[1,3], S.M. Matveev[1,3], D.Yu. Golovin[1], I.A. Vasyukova[1]

[1] Research Institute for Nanotechnologies and Nanomaterials, Derzhavin Tambov State University, Tambov, Russia
[2] Moscow State University, Moscow, Russia
[3] Voronezh State University of Forestry and Technologies named after G.F. Morozov, Voronezh, Russia
E-mail: yugolovin@yandex.ru

Received September 29, 2021
Revised November 17, 2021
Accepted November 18, 2021

The paper presents the results of mechanical properties scanning by means of nanoindentation across the annual growth rings of deciduous trees wood, small-leaved lime (Tilia cordata) and common oak (Quercus robur) in particular. Significant variations in microhardness H and Young's modulus E radial dependencies have been found for any of the studied species. Results can be useful 1) to amend the understanding the nature of macromechanical properties of various wood species and to reveal the details of their formation depending upon microstructural characteristics, 2) to optimize the technologies of growing, reinforcement and subsequent usage of the wood, 3) to develop new independent methods in dendrochronology and dendroclimatology

Keywords: nanocomposites, nanoindentation, nano-/microhardness and Young's modulus scanning, tree annual growth rings, dendrochronology

DOI: 10.21883/TPL.2022.02.52855.19040

In recent years, the entire complex of modern methods and tools routinely used in solid-state physics and material physics has been applied in studies into the structure and properties of wood at all scale and hierarchical levels (nanocrystalline cellulose, elementary nanofibrils, microfibers, cells, annual growth rings). Among these methods are transmission and scanning electron microscopy; atomic force and confocal laser microscopy; X-ray diffraction and computerized tomography; and infrared, Raman, Brillouin, and NMR spectroscopy. Comparative reviews of the capabilities of the most widely used physical methods for examining the molecular, subcellular, and cellular structure of wood have been published recently [1,2].

The mechanical properties of wood at nano- and microscale are studied using the nano/micromechanical testing techniques [3,4], of which nanoindentation (NI) is the most widespread [4–8]. The nano- and micromechanical methods were used to examine the mechanical properties of individual cellulose microfibers [9,10] and cell walls [2,11,12] of various types of wood; a large set of intriguing data was obtained as a result. However, these data characterized specific sites in the structure. The studies did not involve mapping of the mechanical properties of a region encompassing several annual growth rings. Therefore, the relation between the properties of individual microstructural elements of wood and its macromechanical properties determined using traditional techniques [13] remained unexamined.

In the present study, the results of scanning NI of a transverse wood section are reported. This method provided an opportunity to measure and map automatically nano/microhardness H, Young's modulus E, and other local mechanical characteristics at several hundred predefined points on the sample surface. This approach has a number of advantages over traditional techniques for examination of the structure of annual growth rings based on the analysis of images of the transverse section [14]. NI methods allow one to obtain objective data on local physical and mechanical properties with a spatial resolution ranging from several (or several tens of) nanometers to several tens of micrometers and use it for various purposes. Specifically, the obtained data may help i) gain a deeper insight into the nature of macromechanical properties and reveal the micromechanisms of their formation and their dependences on microstructural characteristics; ii) optimize the techniques for growing in the wild and in artificial environments, hardening, and subsequent usage of the wood; iii) develop new independent quantitative methods for dendrochronology and dendroclimatology. The aim of the present study was to reveal annual growth rings and layers of early and late wood and the effective values of E and H in them by NI.

Samples of small-leaved lime (*Tilia cordata*) and common oak (*Quercus robur*) wood were taken in 2020 from 65-year-old trees that grew within the grounds of the Gorel'sk forestry enterprise (Tambov Region). The samples for study were sawed out from transverse sections of wood and dried in a drying chamber in the mild regime at a temperature of 75°C till the loss of sample mass measured during control weighing became zero. The duration of drying performed this way was 24–72 h. The surface preparation involved mechanical grinding and polishing performed using a Buhler (USA) polisher. Roughness R_a of the treated surface was measured with a di Innova (Veeco-Digital Instruments, USA) scanning probe microscope. This roughness was 282 and 162 nm for lime and oak samples, respectively.

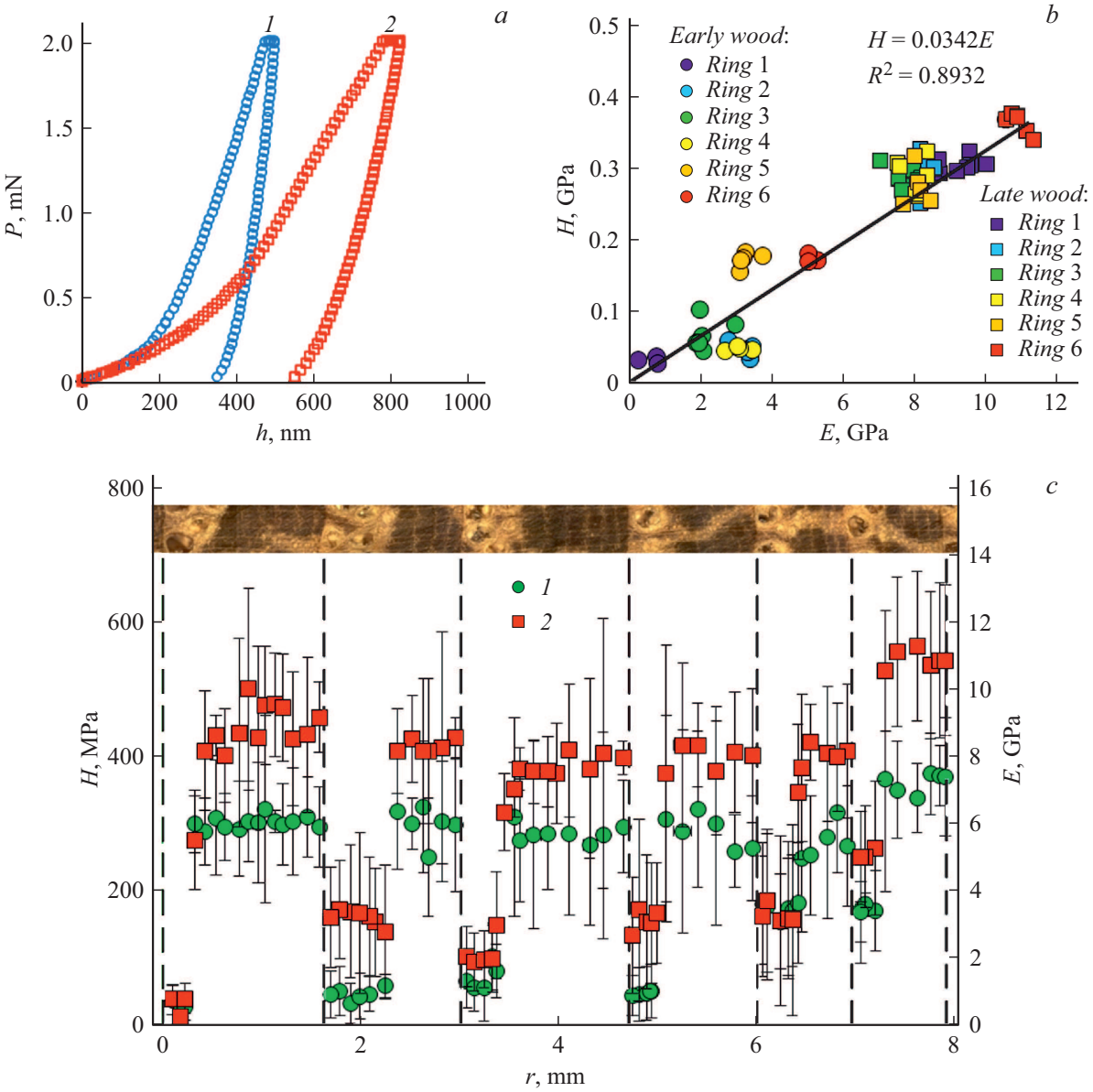

Figure 1. Micromechanical properties of annual growth rings of common oak wood studied by scanning nanoindentation with the maximum load applied to a Berkovich indenter being equal to $P_{max} = 2$ mN. *a* — typical $P-h$ diagrams for late (*1*) and early (*2*) wood; *b* — dependences of hardness H on Young's modulus E for six consecutive annual growth rings; *c* — dependences of H (*1*) and E (*2*) on distance r measured transverse to annual growth rings (for six rings). The structure of wood imaged with an optical microscope is shown in the inset. The boundaries of annual growth rings are indicated with dashed lines. A color version of the figure is provided in the online version of the paper.

The mechanical properties of selected wood samples were mapped using a Hysitron TI-950 (USA) nanoindenter. Measurements were performed in accordance with the recommendations of ISO 14577 and GOST 8.748–2011 for nanoindentation. The maximum load P_{max} applied to an indenter was set to 2 mN. With this load, depth h of indentations was several times higher than roughness parameter R_a, and the lateral size of the deformation zone was on the order of (or somewhat larger than) the crosswise size of a cell. Typical $P-h$ diagrams obtained in experiments on indentation of lime and oak samples are presented in Figs. 1, *a* and 2, *a*. These raw data were processed using the Oliver–Pharr [15] method to retrieve the values of H and E. In view of the relation between the indentation size and the crosswise cell size mentioned above, the H and E values obtained this way may be regarded as effective ones for a certain wood layer (just as the values determined in any macroscopic tests of porous solids such as wood).

The key experimental results on the determination of the radial dependence of H and E in oak and lime are presented in Figs. 1, *c* and 2, *c*, respectively. Each point in these plots is

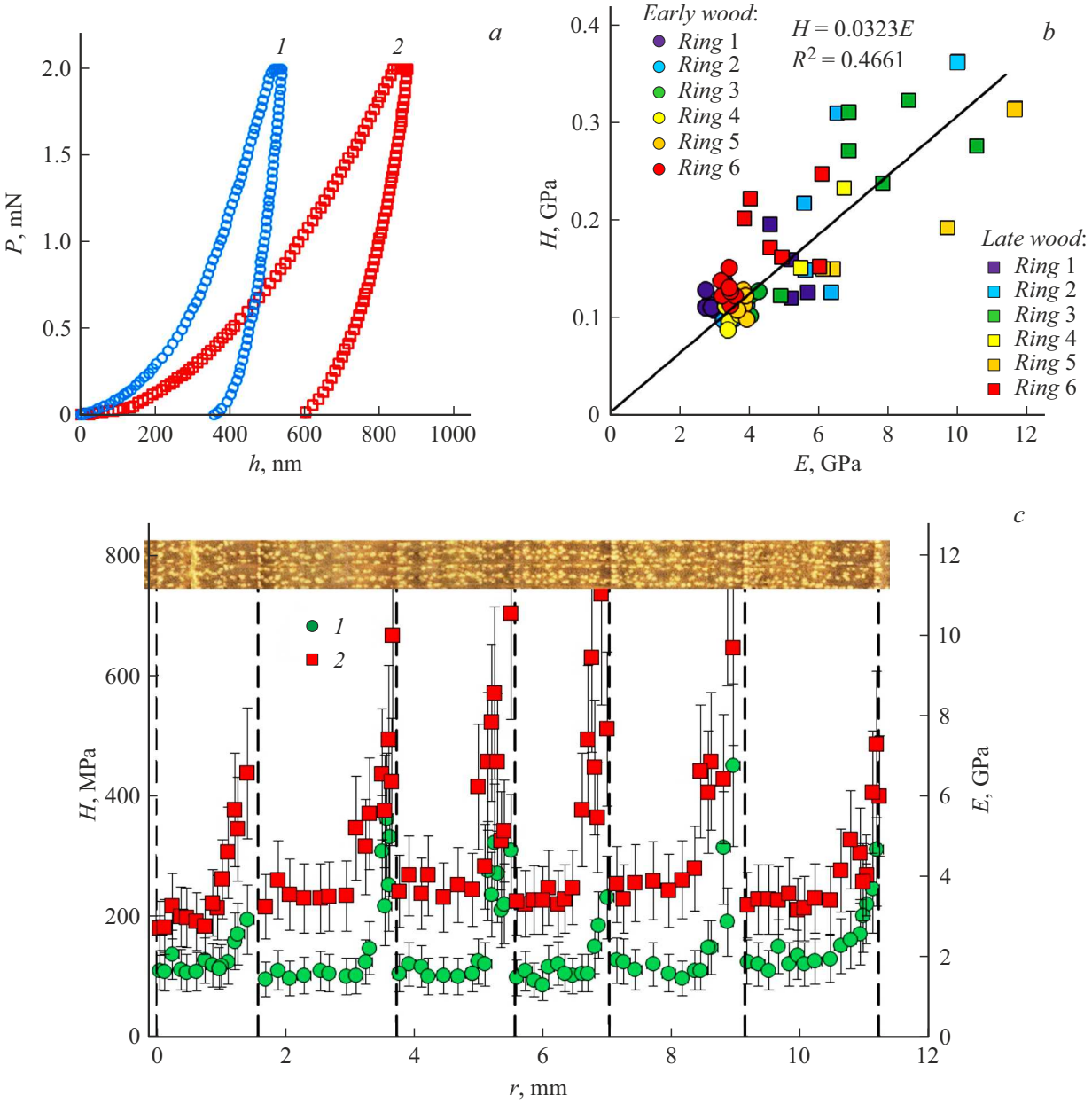

Figure 2. Micromechanical properties of annual growth rings of small-leaved lime wood studied by scanning nanoindentation with the maximum load applied to a Berkovich indenter being equal to $P_{max} = 2$ mN. *a* — typical $P-h$ diagrams for late (*1*) and early (*2*) wood; *b* — dependences of hardness H on Young's modulus E for six consecutive annual growth rings; *c* — dependences of H and E on distance r measured transverse to annual growth rings (for six rings). The structure of wood imaged with an optical microscope is shown in the inset. The boundaries of annual growth rings are indicated with dashed lines. A color version of the figure is provided in the online version of the paper.

the result of averaging over 10–20 individual measurements. „Early" and „late" wood (EW and LW) are traditionally distinguished in the structure of each annual growth ring of any type of wood. Early wood forms in spring and is characterized by low density and hardness values, while late wood formed in summer and autumn has a somewhat higher density and much better mechanical characteristics. The transition from these two structure types may be either abrupt (as in oak, see Fig. 1, *c*) or smooth (as in lime, see Fig. 2, *c*). It can be seen from Figs. 1, *b* and 2, *b* that the values of E and H are correlated in both early and late wood. The difference in mechanical properties at the end stage of growth and at the start of growth in the next year was as large as several hundred percent. This allows one to determine fairly accurately the thickness of rings and the mechanical properties within each ring and then relate them both to yearly variations of the growth conditions and to variations occurring within a growth season. Traditional

Intraring mechanical properties (for the second ring in Figs. 1, *c* and 2, *c*)

Mechanical properties	Oak			Lime		
	Early wood	Late wood	Fraction of EW, %	Early wood	Late wood	Fraction of EW, %
E, GPa	3.2 ± 0.2	8.3 ± 0.2	53	3.7 ± 0.4	6 ± 1	71
H, MPa	45 ± 6	300 ± 20		102 ± 4	230 ± 80	

methods of examination of annual growth rings based on image analysis do not provide such an opportunity.

The differences in mechanical properties of EW and LW in a typical annual growth ring (the second ring in oak and lime) are detailed in the table. It is evident that the Young's modulus in LW is 2.6 times (in oak) or 1.7 times (in lime) higher than E in EW. The hardness values in LW and EW differ even greater: by a factor of 6.5 in oak and 2.2 in lime. Such ratios are, on average, typical of adjacent annual growth rings as well, although the magnitudes of differences in a specific year may deviate substantially from the average ones. For example, the hardness of EW in the fifth and the sixth rings in oak is approximately 3 times higher than H in previous rings, while the hardness of LW remains approximately the same. It is evident that such discrepancies are attributable to the specifics of climatic conditions in these anomalous years. This is also evidenced by the fact that the fifth and the sixth annual growth rings are thinner than the other rings. However, the difference in hardness is much greater than the difference in ring thickness that is used to gauge retrospectively the variations of climatic conditions in traditional dendroclimatology.

It is important to note that the proposed method of scanning without preselection of indentation points and targeting of cell walls, the chosen value of $P_{\max} = 2\,\mathrm{mN}$, and the simplified surface treatment procedure, which leaves a fraction of ground microfibers in capillaries of the sample prepared for measurements, do not preclude one from determining the effective E and H values and even have several advantages over the earlier methods for E and H measurement in individual cell walls at lower $P_{\max}$ (see, e.g., [16], where NI was performed at $P_{\max} = 0.8\,\mathrm{mN}$): i) the method allows for high-throughput inspection of large areas ($\sim 10^4\,\mathrm{mm}^2$ and more) instead of sections several mm^2 in size prepared with a microtome; ii) the ratio of effective microhardness values in LW and EW (with the influence of porosity, capillaries, and their partial filling with ground material taken into account) is much higher than the ratios of E and H in cell walls in LW and EW (see, e.g., [16], where $H_{\mathrm{LW}}/H_{\mathrm{EW}} = 1.07$ and $E_{\mathrm{LW}}/E_{\mathrm{EW}} = 1.4$); iii) the determination of effective E and H values with porosity p taken into account makes them closer to the macrocharacteristics of wood and provides an opportunity to predict those characteristics (if necessary) without the need to determine p independently. The above implies that the measurement of effective H and E values may be a much more sensitive method of dendrochronology and dendroclimatology than the determination based on local H and E values in cell walls and on the measured width variations of annual growth rings.

Thus, it was demonstrated that automated scanning nanoindentation may well augment and expand the capabilities of traditional dendrochronology and dendroclimatology and provide a deeper insight into the mechanisms shaping the mechanical properties of wood via multiscale mapping of such characteristics as hardness and the Young's modulus. Comparing detailed data on the distribution of mechanical characteristics within an annual growth ring and in adjacent growth rings with the data on macrocharacteristics, one may formulate new approaches to the optimization of conditions of production of wood with predetermined mechanical properties. The probable ultimate goal of this is the growth of raw wood (both in the wild and in artificial environments) with high hardness and elasticity parameters and specific acoustic properties.

Acknowledgments

This study was performed at the Common Use Center of the Derzhavin Tambov State University.

Funding

This work was supported by the Russian Science Foundation (grant No. 21-14-00233) and the Ministry of Science and Higher Education of the Russian Federation as part of the project under agreement No. 075-15-2021-709 (unique project identifier RF-2296.61321X0037).

Conflict of interest

The authors declare that they have no conflict of interest.

References

[1] L.A. Donaldson, IAWA J., **40** (4), 645 (2019). DOI: 10.1163/22941932-40190258
[2] E. Toumpanaki, D.U. Shah, S.J. Eichhorn, Adv. Mater., **33** (28), 2001613 (2021). DOI: 10.1002/adma.202001613
[3] *Nanomechanical analysis of high performance materials*, ed. by A. Tiwari (Springer Science+Business Media, Dordrecht–Heidelberg–N.Y.–London, 2014).
[4] Yu.I. Golovin, Phys. Solid State, **63** (1), 1 (2021). DOI: 10.1134/S1063783421010108.

[5] Yu. I. Golovin, Phys. Solid State, **50** (12), 2205 (2008). DOI: 10.1134/S1063783408120019.
[6] Yu.I. Golovin, *Nanoindentirovanie i ego vozmozhnosti* (Mashinostroenie, M., 2009) (in Russian).
[7] A.C. Fischer-Cripps, Nanoindentation (Springer, N.Y., 2011). DOI: 10.1007/978-1-4419-9872-9
[8] N.V. Perepelkin, F.M. Borodich, A.E. Kovalev, S.N. Gorb, Nanomaterials, **10** (1), 15 (2020). DOI: 10.3390/nano10010015
[9] N. Mittal, F. Ansari, V. Krishne Gowda, C. Brouzet, P. Chen, P.T. Larsson, S.V. Roth, F. Lundell, L. Wågberg, N.A. Kotov, L.D. Söderberg, ACS Nano, **12** (7), 6378 (2018). DOI: 10.1021/acsnano.8b01084
[10] *Handbook of nanocellulose and cellulose nanocomposites*, ed. by H. Kargarzadeh, I. Ahmad, S. Thomas, A. Dufresne (Wiley-VCH Verlag, Weinheim, 2017). DOI: 10.1002/9783527689972
[11] S. Cai, S. Hu, Y. Li, X. Wang, Wood Research, **64** (4), 565 (2019). http://www.woodresearch.sk/wr/201904/01.pdf
[12] A.C. Normand, A.M. Charrier, O. Arnould, A.L. Lereu, Sci. Rep., **11**, 5739 (2021). DOI: 10.1038/s41598-021-84994-0
[13] *Handbook of mechanics of materials*, ed. by C.-H. Hsueh, S. Schmauder, C.-S. Chen, K.K. Chawla (Springer Nature, Singapore, 2019). https://www.springer.com/gp/book/9789811068836
[14] J.K. Pearl, J.R. Keck, W. Tintor, L. Siekacz, H.M. Herrick, M.D. Meko, C.L. Pearson, Holocene, **30** (6), 923 (2020). DOI: 10.1177/0959683620902230
[15] W.C. Oliver, G.M. Pharr, J. Mater. Res., **19** (1), 3 (2004). DOI: 10.1557/jmr.2004.19.1.3
[16] P. Mania, M. Nowicki, Bull. Pol. Acad. Sci.: Tech. Sci., **68** (5) 1237 (2020). DOI: 10.24425bpasts.2020.134645